Optimization of Machining Parameters for Cutting AMMC's on Wire Cut EDM using RSM

B. Naga Raju[#1], M. Raja Roy[2], S.Rajesh[3], K.Ramji[4]

[#]*Associate Professor, Mechanical Engineering Department, Anil Neerukonda Institute of Technology and Sciences Sangivalasa, Bheemili, Andhra Pradesh, India 531162*

***Abstract*— The usage of composite materials has been increasing globally in all manufacturing industries. Non-traditional machining methods like electric discharge machining, ultrasonic machining, etc are used to accomplish better results in the machining of composite materials. In the present work, an attempt is made to study the study the effect of Wire Electric Discharge Machining (WEDM) parameters like pulse-on time, pulse-off time and peak current on Surface Roughness(R_a) and Material Removal Rate(MRR) in Aluminum Metal Matrix Composites(AMMCs). The composite material containing aluminum alloy as matrix, silicon carbide as reinforcement is produced by Stir casting technique. Experimentation was conducted in a series of tests called *runs*, in which changes are made in the input variables in order to identify the reasons for changes in the output response using Response Surface Methodology.**

***Keywords*— Wire Cut EDM, Material Removal Rate, Surface Roughness, Response Surface Method.**

I. INTRODUCTION

Machining is an important manufacturing process to obtain various shapes of the components. Over the decades conventional machining has sufficed the requirement of industries. But new exotic work materials as well as innovative geometric design of products and components are putting pressure on capabilities of conventional machining processes to manufacture the components with desired tolerances economically. This has lead to the development of non-conventional manufacturing processes in the industry as efficient and economic alternatives to conventional ones. Wire Electrical Discharge Machining (WEDM) is one of the non-conventional manufacturing processes. As the metal removal is based on complex thermal and chemical phenomena in order to understand its effects on the machined components investigation has been made in this research.

1.1 Electric Discharge Machining (EDM) and Wire EDM

It is probably the most exciting and diversified machine tool developed for this industry in the last fifty years, and has many advantages to offer. Common materials such as tool steel, aluminum, copper, and graphite, to exotic space-age alloys including hastelloy, waspalloy, inconel, titanium, carbide, polycrystalline diamond compacts and conductive ceramics are routinely EDMed.[1,2] The Fig.1.2 shows the CNC Wire EDM and Fig.1.3 shows the Machining in Wire EDM. Fig.1.4 shows a typical block diagram of CNC Wire EDM Machine.

Fig.1.2 CNC Wire Cut EDM

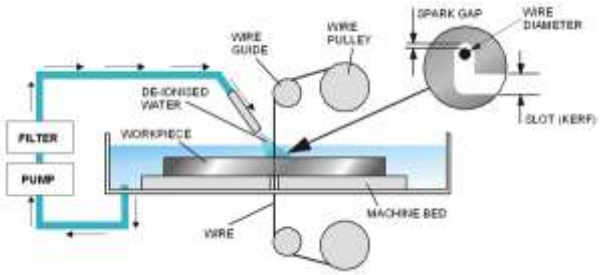

Fig.1.3 Machining in Wire EDM

EDM leaves no residual burrs on the work piece, eliminating secondary de-burring operations that save both time and money. Additionally, EDM leaves no tooling marks, as the surface has a uniform, random pattern compared to marks that are left by grinding and milling operations. Wire EDM also gives designers more latitude in designing dies, and management more control of manufacturing. Parts that have complex geometry and close tolerances don't require you to rely on different skill levels or the use of different machines. Substantial increases in productivity is achieved since the machining is untended, allowing operators to do work in other areas. Most machines run overnight in a "lights-out" environment.

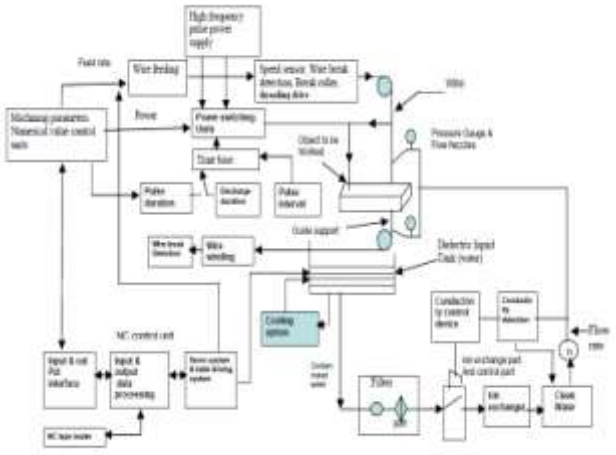

Fig 1.4 A Typical Block Diagram of CNC-Wire EDM Machine

Long running jobs are cut overnight or over the weekend, while shorter jobs are scheduled during the day. Many times, multiple jobs are set up on the worktable and linked together with multiple programs. For example, the die openings and dowel pin holes can be machined on a one-inch thick die block, and when these openings are completed, the machine moves to another location, automatically threads the wire and cut the punches required for the job in a much thicker piece of material.

II LITERATURE REVIEW

Karthikeyan et al [3] investigated the effect of pulse current and pulse duration on electrode wear rate, MRR and SR and also framed a mathematical model and concluded that the current affects the MRR and EWR proportionally, where as an increase in the pulse duration reduces both MRR and EWR.

Mohan et al [4] investigated the machinability study of the Al-SiC composite particle and electrode material on the surface roughness. The results show that the roughness value decreases with an increase in the current and with less SiC particles in the composite.

Suresh Kumar et al [5] carried the experimental investigation to identify the optimal combination of input parameters of electron discharge machining of Al(6351) matrix reinforced with 5wt% silicon carbide(SiC) and 10 wt% boron carbide(B_4C) particles using grey relation analysis. The major input parameters selected to evaluate the process are electrode wear ratio, surface roughness and power consumption, and the corresponding machining parameters are pulse current, pulse on time, pulse duty factor and voltage. Further, ANOVA analysis was carried out to find the contribution of each parameter.

Ramesh et al [6] carried the experimental investigation of Al6061/SiC_p/B_4C_p hybrid MMCs in wire electrical discharge machine. In this study, an attempt is made to study the effect of wire electric discharge machining parameters like voltage, pulse-on time, pulse-off time and current on material removal rate and surface roughness in hybrid metal matrix composites. The results show that increase in silicon carbide leads to decrease in material removal rate and surface finish and addition of boron carbide results decrease in machining performance. It is found that higher pulse on time results in poor the surface finish. It is also found that higher pulse off time resulted in lower surface roughness.

Rajesh et al [7] carried out a comparative study on mechanical properties of SiC and Graphite reinforced Aluminum MMC's. it was found that increasing the SiC content within the aluminum matrix results in significant increase in the UTS, hardness and Young's modulus, but a decrease in the ductility. The percentage of reinforcing particulates in the MMC is varied from 0% to 5% by weight and it was found that the reinforcing particulates beyond 7% and above lead to rejection from the melt.

Kathiresan and Sornakumar [8] conducted EDM studies on Aluminum Alloy Silicon Carbide Composites developed by Vortex Technique and Pressure Die Casting. They studied the effect of variation of SiC on the machinabilitiy characteristics like Surface roughness and MRR of AMMC. The MRR decreases with increase in the percent weight of silicon carbide. The surface finish of the machined work piece improves with percent weight of silicon carbide. The Material Removal Rate (MRR) and Surface roughness of the work piece increases with increase in the current. They did not include in their study the effect of pulse duration, pulse on and pulse off times on mach inability characteristics. Surface roughness is an important measure of the technological quality of a product and a factor that greatly influences manufacturing cost. Quality of the surface plays a very important role in manufacturing the components. A good quality surface significantly improves fatigue strength, corrosion resistance, creep life and wear resistance [9-12]. In addition, surface roughness also affects surface friction, light reflection, ability of holding a lubricant, electrical and thermal contact resistance [13].

III EXPERIMENTAL WORK

3.1 Manufacturing of Composites Using Stir Casting Technique

In the present work, aluminum alloy and 5% wt SiC were die casted, using LM 24 aluminum alloy as matrix material and silicon carbide particles of average size 50 microns as a reinforcement material. The aluminum was melted in a graphite crucible at a controlled temperature. The graphite stirrer was introduced into the crucible to perform mixing process when the molten temperature reached 850^0C. The stirring was carried out for 45 minutes at the rate of 200 rpm. Silicon carbide particles were preheated to 200^0C and introduced into the vortex created in the molten alloy. Here, the crucial thing is to create good wetting between the particulate reinforcement and the liquid aluminum alloy melt. The simplest and most commercially used technique is known as vortex technique or stir-casting technique. The vortex technique involves the introduction of pre-treated

SiC particles into the vortex of molten alloy created by the rotating impeller. The molten slurry is poured into the mould and is allowed to cool in air. The AMMC of size 200x70x7mm^3 was prepared for conducting experiments on WEDM as shown in Fig.3.1.

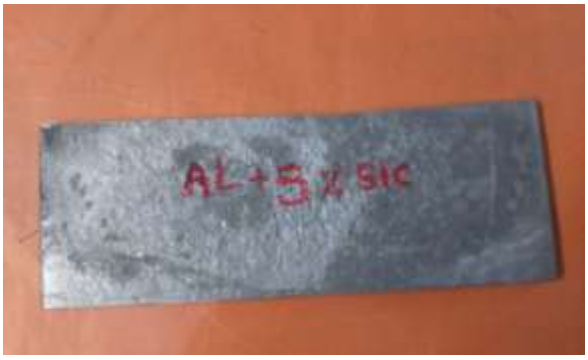

Fig. 3.1 Aluminum with 5% SiC prepared Metal Matrix composite

3.2 Experiments for Evaluating Machinability Characteristics on WEDM

The experiments were conducted on a five axis high precision CNC-Wire Electrical Discharge Machine, model number ULTRACUT 843, manufactured by Electronica Machine Tools, India, shown in Fig.3.2. The basic parts of WEDM machine consists of wire, a work table, a servo control system, a power supply system and dielectric supply system, shown in Fig.3.3.

WEDM consists of several control variables such as pulse-on time, pulse-off time, peak current, wire feed rate, servo reference voltage, wire tension, and dielectric flow rate. The dimensions of the work piece and material also influence the process. Based on the literature survey and operator's experience, the variables such as pulse on time, pulse off time, and peak current were considered as decision (control) variables as shown in Table.3.1.

Each an experiment was performed, with a particular set of input parameters were chosen and work piece (Al with 5% SiC Metal Matrix Composite) was cut with a dimension of 10mmx10mm, whose thickness is 7mm. The machined specimen and the pieces removed from specimen shown in Fig.3.4 and Fig.3.5

Fig.3.2 CNC-Wire Electrical Discharge Machine, model number ULTRACUT

Fig 3.3 – Controller with monitor

Table 3.1 Input parameter levels

S.No	Parameters	Symbol	Levels		
			1	2	3
1	Pulse-on time (micro secs)	T_{on}	100	105	108
2	Pulse-off time (micro secs)	T_{off}	45	50	55
3	Peak current (amp)	Ip	10	11	12

Fig. 3.4 Aluminium metal matrix after machining 10mm slots

Fig. 3.5 Pieces removed from specimen

3.3 Measurement of Surface Roughness

Surface Roughness has been measured by using surface roughness tester as show in Fig.3.6. Surface roughness values tabulated in Table 3.2 are the average values of surface roughness at 3 different locations.

Fig. 3.6 Surface roughness tester

3.4 Calculation of MRR

Material Removal Rate (MRR) is calculated as the ratio of amount of material removed to the time in which material is removed.[15]

$MRR = (2W_g + D) * t * V_c \ mm^3/min$

Where:

W_g = Spark gap,

D = diameter of the wire = 0.25mm

t = Thickness of the work piece in mm

V_c = Cutting speed in mm/min

The cutting speed data (V_c, mm/min) is directly displayed on computer monitor of the machine tool. From this data, MRR is calculated and the values are tabulated in Table 3.2.

Table 3.2 - Experimental Data

S.No	Pulse-on	Pulse-off	Peak current	Ra (microns)	MRR (mm^3/min)
1	100	45	10	1.1947	0.5237
2	100	45	11	1.2094	0.5282
3	100	45	12	1.2743	0.5647
4	100	50	10	1.0582	0.6358
5	100	50	11	1.0668	0.668
6	100	50	12	1.1152	0.7206
7	100	55	10	0.9418	0.8095
8	100	55	11	0.9561	0.8731
9	100	55	12	0.9816	0.8788
10	105	45	10	1.4551	0.3823
11	105	45	11	1.5008	0.3986
12	105	45	12	1.5178	0.3999
13	105	50	10	1.2501	0.4793
14	105	50	11	1.3361	0.5021
15	105	50	12	1.3643	0.5455
16	105	55	10	1.0769	0.6302
17	105	55	11	1.0971	0.6667
18	105	55	12	1.1061	0.6706
19	108	45	10	1.5267	0.2519
20	108	45	11	1.6186	0.2725
21	108	45	12	1.6394	0.2727
22	108	50	10	1.3305	0.3727
23	108	50	11	1.3754	0.4129
24	108	50	12	1.4488	0.4144
25	108	55	10	1.224	0.4948
26	108	55	11	1.2343	0.4956
27	108	55	12	1.3022	0.4979

IV RESUTS AND DISCUSSIONS

4.1 Response Surface Methodology

Response surface methodology uses statistical models, and therefore practitioners need to be aware that even the best statistical model is an approximation to reality. In practice, both the models and the parameter values are unknown, and subject to uncertainty on top of ignorance. Of course, an estimated optimum point need not be optimum in reality, because of the errors of the estimates and of the inadequacies of the model. Nonetheless, response surface methodology has an effective track-record of helping researchers improve products and services: For example, Box's original response-surface modeling enabled chemical engineers to improve a process that had been stuck at a

saddle-point for years. The engineers had not been able to afford to fit a cubic three-level design to estimate a quadratic model, and their biased linear-models estimated the gradient to be zero. Box's design reduced the costs of experimentation so that a quadratic model could be fit, which led to a (long-sought) ascent direction [14].

4.2 Mathematical model of Response Surface Methodology

The Response Surface is described by an second order polynomial equation of the form

$$Y = \beta_0 + \sum_{i=1}^{k} \beta_i x_i + \sum_{i=1}^{k} \beta_{ii} x_{i^2} + \sum \sum_{i<j} \beta_{ij} x_i x_j + \epsilon$$

Y is the corresponding response
(1,2, . . . , S) are coded levels of S quantitative process variables,
The terms are the second order regression coefficients, Second term is attributable to linear effect, Third term corresponds to the higher-order effects, Fourth term includes the interactive effects, The last term indicates the experimental error.

4.3 Mathematical Relationship between the Input Parameters and Surface Roughness

The mathematical relationship for correlating the Surface Roughness and the considered process variables has been obtained as follows.

R_a = -11.87 + 0.210 Ton + 0.0653 Toff - 0.164 IP - 0.000686 Ton*Ton + 0.000369 Toff*Toff + 0.0010 IP*IP - 0.001111 Ton*Toff + 0.00259 Ton*IP - 0.00180 Toff*IP
The Table 4.1 gives the comparison of R_a predicted values with experimental values.

Table 4.1 R_a predicted values compared with experimental

Ton	Toff	IP	Ra	Ra Predicted	%Error
100	45	10	1.195	1.1994	-0.39351
100	45	11	1.209	1.2346	-2.08213
100	45	12	1.274	1.2718	0.194862
100	50	10	1.058	1.0556	0.24154
100	50	11	1.067	1.0818	-1.40989
100	50	12	1.115	1.1101	0.457944
100	55	10	0.942	0.9303	1.216566
100	55	11	0.956	0.9476	0.893655
100	55	12	0.982	0.9668	1.505226
105	45	10	1.455	1.4261	1.995676
105	45	11	1.501	1.4742	1.774531
105	45	12	1.518	1.5243	-0.43025
105	50	10	1.25	1.2545	-0.35334
105	50	11	1.336	1.2936	3.17785
105	50	12	1.364	1.3348	2.160824
105	55	10	1.077	1.1014	-2.27774
105	55	11	1.097	1.1316	-3.14185
105	55	12	1.106	1.1638	-5.21336
108	45	10	1.527	1.5456	-1.2379
108	45	11	1.619	1.6015	1.058816
108	45	12	1.639	1.6594	-1.21877
108	50	10	1.331	1.3574	-2.02054
108	50	11	1.375	1.4043	-2.09851
108	50	12	1.449	1.4532	-0.30358
108	55	10	1.224	1.1876	2.971968
108	55	11	1.234	1.2255	0.711376
108	55	12	1.302	1.2655	2.820503

4.3.1 Normal Probability Plot for Ra

The normal probability plot as shown in Fig: 4.1 represents a clear pattern (as the points are almost in a straight line) indicating that all the factors and their interaction given in are affecting the Ra. In addition, the errors are normally distributed and the regression model is well fitted with the observed values

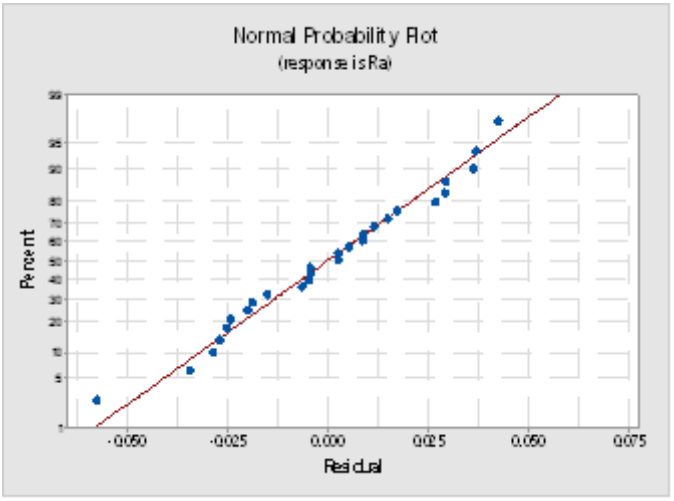

Fig: 4.1 Normal Probability Plot for Ra

4.3.2 Standardized Residual Vs Fitted Value for Surface Roughness

Fig: 4.2 indicate that the maximum variation which shows the high correlation that exists between fitted values and observed values.

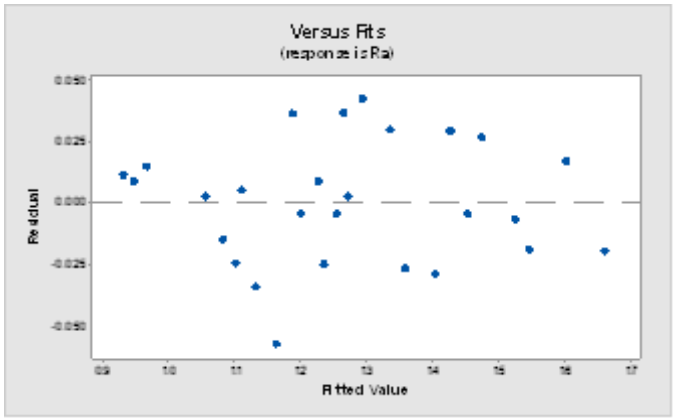

Fig: 4.2 Residual Vs Fitted Value for Surface Roughness

4.3.3 Effect Of Input Parameters

Fig: 4.3 Main Effects plot for Ra

4.3.4 Interaction Effects

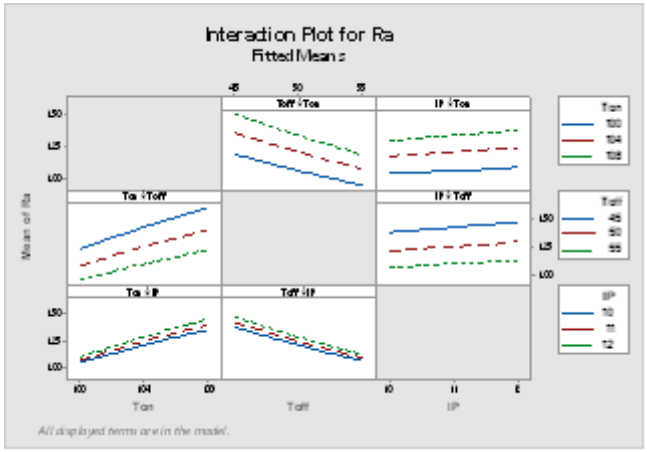

Fig: 4.4 Interaction Effects plot for Ra

4.4 Mathematical Relationship between the Input Parameters and Metal Removal Rate

The mathematical relationship for correlating the Metal removal rate and the considered process variables has been obtained as follows

MRR = -19.05+ 0.3077 Ton + 0.1068 Toff + 0.382 IP- 0.001266 Ton*Ton+ 0.000242 Toff*Toff- 0.00501 IP*IP- 0.001056 Ton*Toff - 0.00266 Ton*IP + 0.000557 Toff*IP

The Table 4.2 gives the comparison of MRR predicted values with experimental values.

Table 4.2 MRR predicted values compared with experimental

Ton	Toff	IP	MRR	MRR Predicted	% Error
100	45	10	0.5237	0.50188	4.1662
100	45	11	0.5282	0.53703	-1.672
100	45	12	0.5647	0.56217	0.4485
100	50	10	0.6358	0.65052	-2.315
100	50	11	0.668	0.68845	-3.062
100	50	12	0.7206	0.71637	0.5866
100	55	10	0.8095	0.81128	-0.22
100	55	11	0.8731	0.85200	2.4171
100	55	12	0.8788	0.88270	-0.444
105	45	10	0.3823	0.37192	2.7148
105	45	11	0.3986	0.39375	1.2165
105	45	12	0.3999	0.40557	-1.418
105	50	10	0.4793	0.49415	-3.098
105	50	11	0.5021	0.51876	-3.319
105	50	12	0.5455	0.53336	2.2246
105	55	10	0.6302	0.62850	0.2696
105	55	11	0.6667	0.65590	1.6203
105	55	12	0.6706	0.67328	-0.4
108	45	10	0.2519	0.26356	-4.628
108	45	11	0.2725	0.27740	-1.797
108	45	12	0.2727	0.28122	-3.126
108	50	10	0.3727	0.36994	0.7402
108	50	11	0.4129	0.38656	6.3786
108	50	12	0.4144	0.39317	5.1222
108	55	10	0.4948	0.48845	1.2841
108	55	11	0.4956	0.50785	-2.472
108	55	12	0.4979	0.51725	-3.885

4.4.1 Normal Probability Plot for MRR

The normal probability plot in the Fig: 4.5, shows a clear pattern (as the points are almost in a straight line) indicating that all the factors and their interaction given in are affecting the MRR. In addition, the errors are normally distributed and the regression model is well fitted with the observed values.

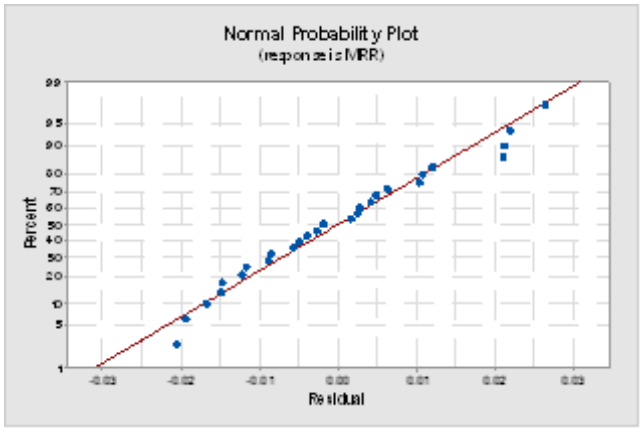

Fig: 4.5 Normal Probability Plot for MRR

4.4.2 Standardized Residual Vs Fitted Value For MRR

Fig: 4.6 indicate that the maximum variation which shows the high correlation that exists between fitted values and observed values.

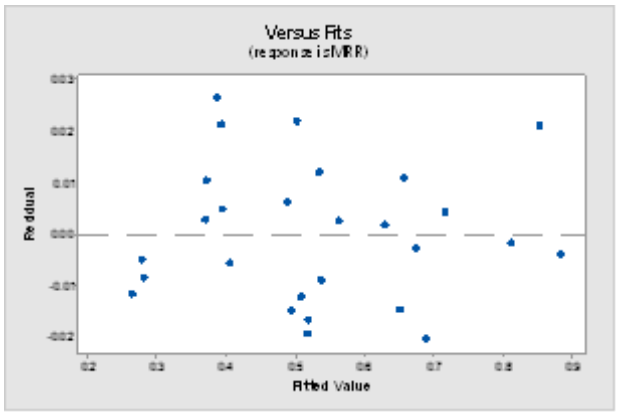

Fig: 4.6 Residual Vs Fitted Value For MRR

4.4.3 Effect of Input Parameters

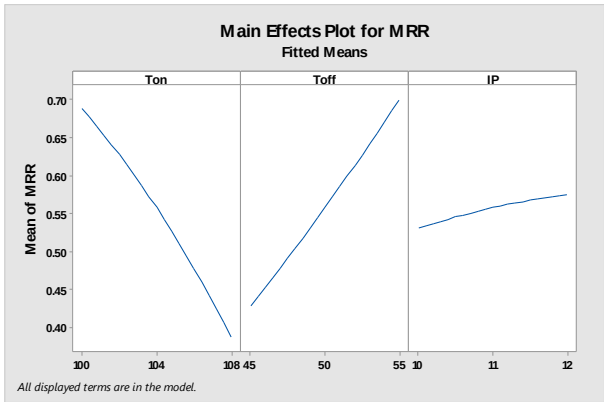

Fig: 4.7 Main Effects plot for MRR

4.4.4 Interaction Effects

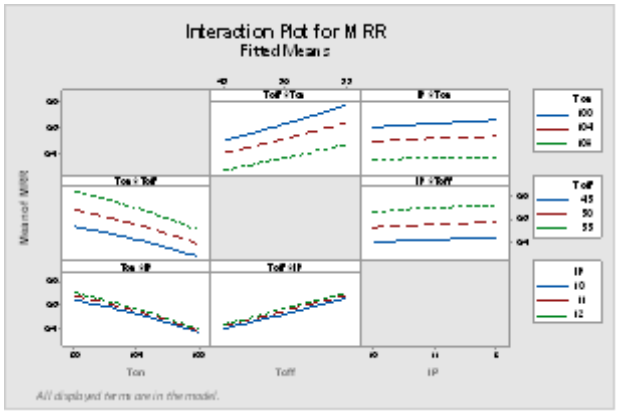

Fig: 4.8 Interaction Effects plot for MRR

4.5 Optimisation Plot:

A Minitab Response Optimizer tool shows how different experimental settings affect the predicted responses for factorial, response surface, and mixture designs. Minitab calculates an optimal solution and draws the plot. The optimal solution serves as the starting point for the plot. This optimization plot allows to interactively changing the input variable settings to perform sensitivity analyses and possibly improve the initial solution.

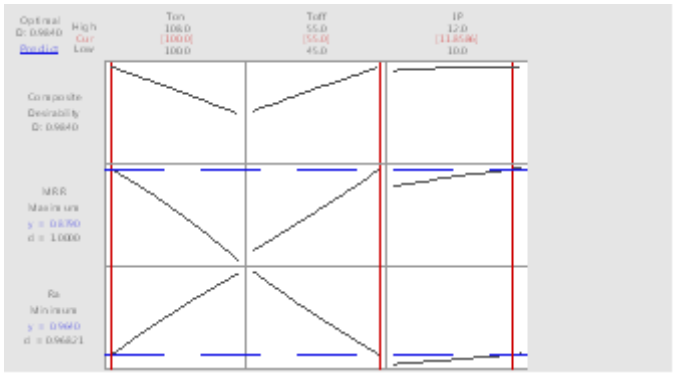

Fig: 4.9 Optimisation plot for MRR and Surface Roughness

The optimization plot as shown in Fig:4.9 signifies the affect of each factor (columns) on the responses or composite desirability (rows). The vertical red lines on the graph represent the current factor settings. The numbers displayed at the top of a column show the current factor level settings (in red). The horizontal blue lines and numbers represent the responses for the current factor level. Minitab calculates the maximum metal removal rate and minimum surface roughness.

From the optimization plot it can be said that the maximum metal removal rate is 0.8790 mm^3/min and the minimum surface roughness is 0.9640µm obtained when Ton=100 µs, Toff=55 µs, and IP=11.86A.

V. CONCLUSION

In the present work, Multi-Response Optimization problem has been solved by using an optimal parametric combination of input parameters such as Pulse on Time, Pulse off Time and Input Voltage. These optimal parameters ensures in producing high surface quality turned product.

Response Surface Methodology is successfully implemented for optimizing the input parameters.

This paper produces a direct equation with the combination of controlled parameters which can be used in industries to know the Values of MRR and Surface Roughness instead of machining.

Hence we conclude that the optimal solution for maximum metal removal rate is 0.8790 mm^3/min and the minimum surface roughness is 0.9640µm obtained when Ton=100 µs, Toff=55 µs, and IP=11.86A.

REFERENCES

[1] M. A. Taha. 2001. Practicalization of cast metal matrix composites. Materials and Design, Vol. 22, no. 6, pp.431-441.

[2] J. Peronczyk. and J. Kozak. 1998. Electrical discharge machining (EDM) of the metal matrix composites (MMC). In: Proceedings of the 8th International Conference on Rotary Fluid-flow Machines. p. 391, Rzeszow-Bystre, Krakow, Poland.

[3] R. Karthikeyan, P. R. Lakshmi Narayanan, and R. S. Nagarazan, "Mathematical modelling for electric discharge machining of aluminium-silicon carbide particulate composites," Journal of Materials Processing Technology, vol. 87, no. 1–3, pp. 59–63, 1999.

[4] B. Mohan, A. Rajadurai, and K. G. Satyanarayana, "Effect of SiC and rotation of electrode on electric discharge machining of Al-SiC composite," Journal of Materials Processing Technology, vol. 124, no. 3, pp. 297–304, 2002."

[5] S. Suresh Kumar, M. Uthayakumar, S. Thirumalai Kumaran, P. Parameswaran, and E. Mohandas "Electrical Discharge Machining of Al (6351)-5% SiC-10% B4C Hybrid Composite: A Grey Relational Approach" Journal of Modelling and Simulation in EngineeringVolume 2014 (2014), Article ID 426718.

[6] S.Ramesh, N.Natarajan, V.Krishnaraj "Experimental investigation of Al6061/SiC_p/B_4C_p hybrid MMCs in wire electrical discharge machine" Indian Journal of Engineering & Material Sciences, Vol.21, pp.409-417, 2014.

[7] Rajesh.S, A.Gopla Krishna, P.Rama Murthy Raju, D.Kondayya "Comparative study on Mechanical Properties of SiC and Graphite reinforced Aluminium MMCs" Proceedings of International Conference on Materials Processing and Characterization, 8th -10th March 2012.

[8] M.Katiresan and T.Sornakumar "EDM studies on Aluminium Alloy Silicon Carbide Composites developed by Vortex Technique and Pressure Die Casting" Journal of Minerals & Materials & Engineering, Vol.9,No.1,pp.79-88,2010.

[9] Guu Y. H. and Hocheng H. 2001. Improvement of fatigue life of electrical discharge machined AISI D2 tool steel by TiN coating. Mater Sci Eng A, pp. 155-162, Vol. 318.

[10] Jeelani S. and Collins M.R. 1988. Effect of electrical discharge machining on the fatigue life of Inconel 718. Int J. Fatigue, pp. 121-125, Vol. 10.

[11] Zeid O.A.A. 1997. On the effect of electro discharge machining parameters on the fatigue life of AISI D6 tool steel. J Mater Process Technol., pp. 27-32, Vol. 68.

[12] Ramulu A., Paul G and Patel J. 2001. EDM surface effects on the fatigue strength of a 15 vol% SiC/Al metal matrix composite material, Compos Struct., pp. 79-86, Vol. 54.

[13] Rashid Ab., Gan M.F.F. and Muhammad N.Y. 2009. Mathematical modeling to predict surface roughness in CNC Milling. World Academy of Science Engineering and Technology. pp. 393-396, Vol. 53.

[14] Nuran Bradley; The Response Surface Methodology, Indian University of south bend, 2007.